Dynamics Model of a Four-Wheeled Mobile Robot for Control Applications – A Three-Case Study

Chapter · January 2014

DOI: 10.1007/978-3-319-11310-4_10

1 author:

Maciej Trojnacki
PIAP Space sp. z o.o.
97 PUBLICATIONS **185** CITATIONS

SEE PROFILE

Dynamics Model of a Four-Wheeled Mobile Robot for Control Applications – A Three-Case Study

Maciej Trojnacki

Industrial Research Institute for Automation and Measurements PIAP, Warsaw, Poland
mtrojnacki@piap.pl

Abstract. The problem of dynamics modeling of a four-wheeled mobile robot is analyzed in this paper. All wheels of the robot are non-steered and the servomotors are used for driving the robot. Three cases of the robot drive system are considered. In the first case, two out of four wheels of the robot are independently driven, i.e., a pair of front or rear wheels. In the second case, the same wheels of the robot are driven but drive is also transmitted to the remaining wheels via toothed belts at each side of the robot. Finally, in the third case all four wheels are independently driven. Kinematic structure of the robot and its kinematics are described. The dynamics model of the robot dedicated for control applications is derived. It takes into account tire-ground contact conditions and wheel slips. The tire-ground contact conditions are characterized by coefficients of friction and rolling resistance. A simple form of the tire model, which considers only the most important effects of tire-ground interaction, is applied. The robot dynamics model also includes the presence of friction in kinematic pairs and the electromechanical model of servomotor drive unit. The presented robot dynamics model can be used for simulation-based investigations of control systems under development. Because the model was also formulated in a form linear with respect to parameters, it is possible to use it as a part of the robust or adaptive type control system.

Keywords: wheeled mobile robot, wheel slip, dynamics model, tire model, drive unit model, model of friction in kinematic pairs.

1 Introduction

Wheeled mobile robots are the vehicles whose motion is a result of interaction of wheels with the ground. An important problem associated with interaction of wheels with the ground is the slip phenomenon. Although this problem is a well-known subject of research in the automotive field (representative examples of works can be [10, 18]), in case of wheeled robots it is often neglected. Moreover, wheels of wheeled robots usually have different geometry and properties in comparison to car wheels. Robotic wheels often have non-pneumatic tires, which demands realization of dedicated investigations. This topic of research seems to be rather rare in the literature. One example of works oriented to non-pneumatic small-size robotic tires is [2].

Neglecting wheel slip in case of wheeled mobile robots is reasonable, when robot moves with small speeds and accelerations which results in longitudinal slips of

D. Filev et al. (eds.), *Intelligent Systems'2014*,
Advances in Intelligent Systems and Computing 323, DOI: 10.1007/978-3-319-11310-4_10

limited magnitude. In turn, neglecting of side slips can be justified, when robot moves with small speeds, has steered or caster wheels and turning radius is large with respect to velocity of motion. However, many authors assume lack of slip a priori, that is, without any reference to conditions of robot motion and without analysis of validity of this assumption.

It is worth emphasizing that in case of wheeled robots with all non-steered wheels, which is the most popular design type in commercial solutions so far (see e.g. [6]), the phenomenon of slip is the inherent property of their motion. Robots like that are called skid-steered mobile robots and are objects of research, for example, in the works [7, 16]. In case of those robots, the side components of ground reaction forces are taken into account with aid of simple models of wheel-ground interaction, for example in [7]. As a rule, the occurrence of self-aligning moment during turning of the wheel is not considered.

With all of the above taken into account, wheeled mobile robots can be divided in two groups: (1) robots for which in typical operating conditions there is almost no wheel sliding during motion, and (2) robots for which wheel sliding is an inherent feature of motion.

Robots with steered or caster wheels belong to the first group. They are usually intended for use inside buildings (indoor robots). An example of such a design is the popular Pioneer 2-DX robot shown in Fig. 1a.

The second group is comprised of robots with all wheels non-steered. Usually robots like that are intended for use in open terrain (outdoor robots). Example of this kind of design is the IBIS robot shown in Fig. 1b [19], developed by the Industrial Institute for Automation and Measurements PIAP.

a) b)

Fig. 1. Examples of wheeled mobile robots: a – Pioneer 2-DX, b – IBIS [19]

In case of wheeled robots from the second group, motion of robot body is not defined by a kinematic dependency on rotation of driven wheels, as it is in the case of robots from the first group. This difference is associated with occurrence of wheel sliding always during change of direction of motion. In this case, forces generated between tire tread and ground depend in a non-linear manner on various factors, e.g.: material and shape of the tread and of the ground, velocity of tire tread with respect to ground, etc.

In typical robot operating conditions, some of the factors connected with the ground may change in rather arbitrary fashion. For this reason, it is impossible to find

analytical expression that would allow to associate desired motion of robot body with motion parameters of driven wheels necessary to its realization, and would be valid in any conditions.

The phenomenon of slip is connected with type of ground on which the wheel moves. It is clear that wheel moving on a ground surface made of concrete will behave in a different way than the same wheel on ice. In the latter case one will expect the occurrence of much larger wheel slips on average for the identical maneuver. Research concerning robot motion on various types of ground is the topic, for instance, of work [16].

Wheeled mobile robots are vehicles that should move along desired trajectories. As far as control of wheeled mobile robots is concerned, usually robot motion without wheel slips and on the ground with homogenous properties is assumed, which is reflected e.g. in [3, 4, 11]. The works in which the tracking control algorithms take into account wheel slips and/or diverse ground properties can be found as well. Among others there are [8, 13, 17] and [5, 7, 16] in which the authors examine the effect of diverse ground properties on the movement realized by the robot. The problem of control of the skid-steered mobile robots is in particular considered in the works [1, 7, 16] in which wheel slips are included in the control algorithm. Occurrence of the wheel slip is also taken into account, for instance, in the control algorithm of an off-road agricultural vehicle [8].

Because of the mentioned problems, in this work model of a four-wheeled skid-steered mobile robot including wheel slips will be presented. This model can be used for simulation-based investigations of control systems under development. Because the model is also formulated in the form linear with respect to parameters it may be included in the structure of robust or adaptive control systems.

2 Model of the Robot

In this paper dynamics model of the four-wheeled robot including wheel slips is derived. All wheels of the robot are non-steered and the servomotors are used for driving. Three cases of the robot drive system are taken into consideration:

- two out of four wheels of the robot are independently driven, that is, front or rear pair of wheels,
- the same wheels as in the previous case are driven, but in addition drive is transmitted to the remaining two wheels via two toothed belts (tracks), one on each side of the robot,
- all four wheels are independently driven.

2.1 Robot Kinematics

Kinematic structure of the robot and distribution of the velocity vectors are shown in Fig. 2. It is possible to distinguish the following main components of the robot: 0 – mobile platform, 1-4 – wheels, 5-6 – toothed belts.

The following designations for the i^{th} wheel have been introduced in the robot model: A_i – geometric center, r_i – geometric (unloaded) radius, θ_i – spin angle.

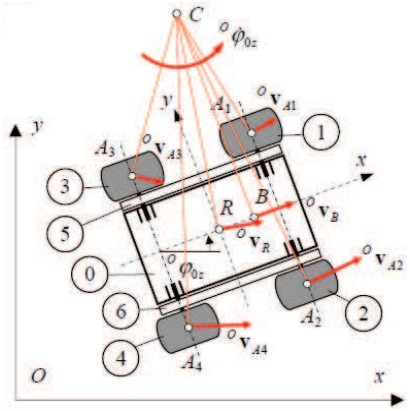

Fig. 2. Kinematic structure of the robot ($A_1A_3 = A_2A_4 = L$, $A_1A_2 = A_3A_4 = W$)

It is assumed that robot motion is realized in Oxy plane of the fixed coordinate system $\{O\}$. The moving coordinate system, considered as rigidly connected to the robot, is denoted with symbol $\{R\}$. Position and orientation of the mobile platform are described by the vector of generalized coordinates:

$$ {}^{O}\mathbf{q} = [{}^{O}x_R,\ {}^{O}y_R,\ {}^{O}\varphi_{0z}]^T, \tag{1} $$

where: ${}^{O}x_R$, ${}^{O}y_R$ are coordinates of point R belonging to the mobile platform, and ${}^{O}\varphi_{0z}$ denotes angle of rotation of mobile platform about Oz axis with respect to the fixed coordinate system $\{O\}$.

In turn, vectors of generalized velocities respectively in $\{O\}$ and $\{R\}$ coordinate systems can be written as:

$$ {}^{O}\dot{\mathbf{q}} = \left[{}^{O}\dot{x}_R,\ {}^{O}\dot{y}_R,\ {}^{O}\dot{\varphi}_{0z}\right]^T,\ {}^{R}\dot{\mathbf{q}} = \left[{}^{R}\dot{x}_R^O,\ {}^{R}\dot{y}_R^O,\ {}^{R}\dot{\varphi}_{0z}^O\right]^T, \tag{2} $$

where: ${}^{O}v_{Rx} = {}^{O}\dot{x}_R$, ${}^{O}v_{Ry} = {}^{O}\dot{y}_R$, ${}^{R}v_{Rx}^O = {}^{R}\dot{x}_R^O$, ${}^{R}v_{Ry}^O = {}^{R}\dot{y}_R^O$.

Those two vectors satisfy the relationship:

$$ {}^{O}\dot{\mathbf{q}} = {}^{O}\mathbf{J}^{R}\ {}^{R}\dot{\mathbf{q}}, \tag{3} $$

where matrix ${}^{O}\mathbf{J}^{R}$ has the following form:

$$ {}^{O}\mathbf{J}^{R} = \begin{bmatrix} \cos\left({}^{O}\varphi_{0z}\right) & -\sin\left({}^{O}\varphi_{0z}\right) & 0 \\ \sin\left({}^{O}\varphi_{0z}\right) & \cos\left({}^{O}\varphi_{0z}\right) & 0 \\ 0 & 0 & 1 \end{bmatrix}. \tag{4} $$

If one makes assumption that ${}^{R}v_{Ry}^{O} = 0$, then vector of generalized velocities ${}^{O}\dot{\mathbf{q}}$ can be defined on the basis of kinematic equations of motion in the form:

$$ {}^{O}\dot{\mathbf{q}} = \begin{bmatrix} {}^{O}\dot{x}_R \\ {}^{O}\dot{y}_R \\ {}^{O}\dot{\varphi}_{0z} \end{bmatrix} = \begin{bmatrix} \cos({}^{O}\varphi_{0z}) & 0 \\ \sin({}^{O}\varphi_{0z}) & 0 \\ 0 & 1 \end{bmatrix} \begin{bmatrix} {}^{R}v_{Rx}^{O} \\ {}^{R}\dot{\varphi}_{0z}^{O} \end{bmatrix}, \tag{5} $$

where vector ${}^{R}\mathbf{v} = [{}^{R}v_{Rx}^{O}, {}^{R}\dot{\varphi}_{0z}^{O}]^T$ contains respectively component of velocity of the point *R* of the robot on the *Rx* direction of $\{R\}$ coordinate system and the yaw rate of the mobile platform.

The above equation is valid in case when the robot moves on a horizontal ground.

Point *C* in Fig. 2 is the instantaneous center of rotation of the robot frame. Projection of this point on *Rx* axis is indicated with point *B*.

The analyzed robot is the nonholonomic system. From distribution of velocity vector of the point *B*, it follows that it is subjected to nonholonomic constraints of the form:

$$ \mathbf{a}\ {}^{O}\dot{\mathbf{q}} = 0, \tag{6} $$

where $\mathbf{a} = [-\sin({}^{O}\varphi_{0z}), \cos({}^{O}\varphi_{0z}), {}^{R}x_C]$ is the vector of nonholonomic constraints.

In turn, projections of velocities of points A_i (i.e., geometric centers of wheels) on *Rx* and *Ry* axes of the $\{R\}$ coordinate system satisfy the relationships [7]:

$$ {}^{R}v_{lx}^{O} = {}^{R}v_{A1x}^{O} = {}^{R}v_{A3x}^{O},\ {}^{R}v_{rx}^{O} = {}^{R}v_{A2x}^{O} = {}^{R}v_{A4x}^{O}, \tag{7} $$

$$ {}^{R}v_{fy}^{O} = {}^{R}v_{A1y}^{O} = {}^{R}v_{A2y}^{O},\ {}^{R}v_{by}^{O} = {}^{R}v_{A3y}^{O} = {}^{R}v_{A4y}^{O}, \tag{8} $$

where: *l* – wheels of the left-hand side ($l = \{1,3\}$), *r* – wheels of the right-hand side ($r = \{2,4\}$), *f* – front wheels ($f = \{1,2\}$), *b* – back wheels ($b = \{3,4\}$).

In case of plane motion of the mobile platform, velocity vector of the point *R* depends on angular velocity ${}^{R}\dot{\varphi}_{0z}^{O}$ and radius of curvature R_z of the path according to the formula:

$$ {}^{R}v_{R}^{O} = {}^{R}\dot{\varphi}_{0z}^{O} R_z, \tag{9} $$

where ${}^{R}v_{R}^{O} = {}^{R}\dot{\varphi}_{0z}^{O} R_z$ is the velocity with which the point *R* moves with respect to the stationary coordinate system $\{O\}$.

In addition, in a general case the acceleration vector ${}^{R}\mathbf{a}_{R}^{O}$ of the point *R*, expressed in the robot coordinate system $\{R\}$, has both tangential and normal components, that is, the following dependencies are valid:

$$ {}^{R}\mathbf{a}_{R}^{O} = {}^{R}\mathbf{a}_{R\tau}^{O} + {}^{R}\mathbf{a}_{Rn}^{O} \quad \Rightarrow \quad {}^{R}\mathbf{a}_{R\tau}^{O} = {}^{R}\mathbf{a}_{R}^{O} - {}^{R}\mathbf{a}_{Rn}^{O}, \tag{10} $$

where ${}^{R}\mathbf{a}_{R\tau}^{O}$ and ${}^{R}\mathbf{a}_{Rn}^{O}$ denote respectively vectors of tangential and normal accelerations of the point *R*.

Thus, for determination of velocity components of the point R, based on the known acceleration vector ${}^{R}\mathbf{a}_{R}^{O}$, the following equations should be used:

$$ {}^{R}\dot{v}_{Rx}^{O}={}^{R}a_{Rx}^{O}+{}^{R}v_{Ry}^{O}\,{}^{R}\dot{\varphi}_{0z}^{O}, \quad {}^{R}\dot{v}_{Ry}^{O}={}^{R}a_{Ry}^{O}-{}^{R}v_{Rx}^{O}\,{}^{R}\dot{\varphi}_{0z}^{O}. \tag{11} $$

Those equations result from projecting acceleration vectors on axes of $\{R\}$coordinate system.

Projections of velocities of points A_i on Rx and Ry axes of the coordinate system $\{R\}$ can be written as functions of generalized velocities in the form:

$$ \begin{bmatrix} {}^{R}v_{lx}^{O} \\ {}^{R}v_{rx}^{O} \\ {}^{R}v_{fy}^{O} \\ {}^{R}v_{by}^{O} \end{bmatrix} = \begin{bmatrix} 1 & -W/2 \\ 1 & W/2 \\ 0 & L/2-{}^{R}x_{C} \\ 0 & -L/2-{}^{R}x_{C} \end{bmatrix} \begin{bmatrix} {}^{R}v_{Rx}^{O} \\ {}^{R}\dot{\varphi}_{0z}^{O} \end{bmatrix} = \begin{bmatrix} 0 & -W/2+{}^{R}y_{C} \\ 0 & W/2+{}^{R}y_{C} \\ 1 & L/2 \\ 1 & -L/2 \end{bmatrix} \begin{bmatrix} {}^{R}v_{Ry}^{O} \\ {}^{R}\dot{\varphi}_{0z}^{O} \end{bmatrix}. \tag{12} $$

Moreover, projections of velocity of the point A_i, which belongs to the i-th wheel, on Rx and Ry axes of $\{R\}$ coordinate system depend on angular velocity of spin of the wheel $\dot{\theta}_i$ and the velocity of slip, that is, the following equations are satisfied:

$$ {}^{R}v_{Aix}^{O}=\dot{\theta}_i\, r_i+{}^{R}v_{Six}^{O}, \; {}^{R}v_{Aiy}^{O}={}^{R}v_{Siy}^{O}, \tag{13} $$

where ${}^{R}v_{Six}^{O}$, ${}^{R}v_{Siy}^{O}$ are components of slip velocity in $\{R\}$ coordinate system, that is, velocity of motion of points of wheel which are in contact with the ground with respect to the ground.

Thus, the generalized velocities can be written in the form:

$$ {}^{R}v_{Rx}^{O}=\left({}^{R}v_{lx}^{O}+{}^{R}v_{rx}^{O}\right)/2, \quad {}^{R}v_{Ry}^{O}=-{}^{R}\dot{\varphi}_{0z}^{O}\,{}^{R}x_{B}, \quad {}^{O}\dot{\varphi}_{0z}=\left({}^{R}v_{rx}^{O}-{}^{R}v_{lx}^{O}\right)/W=\left({}^{R}v_{by}^{O}-{}^{R}v_{fy}^{O}\right)/L, \tag{14} $$

Coordinates of the instantaneous center of rotation C (Fig. 2) can be calculated from dependencies:

$$ {}^{R}x_{C}={}^{R}x_{B}=-{}^{R}v_{Ry}^{O}/{}^{R}\dot{\varphi}_{0z}^{O}, \quad {}^{R}y_{C}={}^{R}v_{Rx}^{O}/{}^{R}\dot{\varphi}_{0z}^{O}. \tag{15} $$

Position of the point B has critical influence on stability of robot motion. If the origin of the coordinate system associated with the robot is situated in the middle of the distance between front and rear wheels, then one may assume that coordinates of the point B should satisfy the relationship:

$$ {}^{R}x_{B}\in(-L/2,\,L/2). \tag{16} $$

2.2 Inverse Kinematics and Tracking Control

In case of tracking control of robot motion, it is necessary to solve the inverse kinematics problem, that is, to determine desired angular velocities of spin of wheels from desired motion of the robot body.

One of possible approaches to tracking control is to make assumption that robot motion is given in the form of vector of generalized velocities ${}^{R}\mathbf{v}_{d} = [{}^{R}v_{Rd}^{O},\ {}^{R}\dot{\varphi}_{0zd}^{O}]^{T}$, which corresponds to desired trajectory of robot motion expressed in the form of vector of desired generalized coordinates ${}^{O}\mathbf{q}_{d} = [{}^{O}x_{Rd},\ {}^{O}y_{Rd},\ {}^{O}\varphi_{0zd}]^{T}$. Then, for tracking control of robot motion it is possible to apply the wheels' velocity controller. This approach is illustrated in Fig. 3.

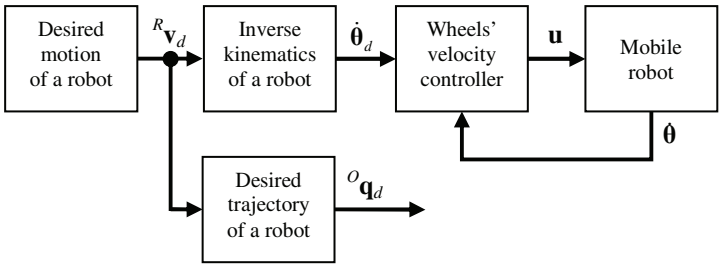

Fig. 3. Schematic diagram of robot motion control system with only controller of wheels' velocity

One should consider that motion of the analyzed robot is highly affected by the occurring wheel slips. In case of longitudinal motion of the robot, when body is in translational motion, and wheels in plane motion, if wheel slips are small, then it is possible to determine angular velocities of spin of the driven wheels required to realize the motion with desired velocity of the point *R* (i.e. to solve the inverse kinematics problem for the analyzed case) using the formula:

$$\dot{\theta}_{id} = {}^{R}v_{Rd}^{O} / r_{i}\,. \tag{17}$$

The situation becomes much more complex, when robot negotiates a curve or turns in place. Because robot wheels are non-steered, its motion depends on longitudinal forces, and also to large extent on lateral forces, that is, on robot dynamics in general.

In this case, because of action of lateral forces, the robot will rotate about the vertical axis with smaller angular velocity ${}^{R}\dot{\varphi}_{0z}^{O}$ than it follows from imposed angular velocities of wheels $\dot{\theta}_{ld}$ and $\dot{\theta}_{rd}$ as calculated based on laws of kinematics.

The difference will be the more pronounced, the smaller the number of driven wheels, because of smaller ratio of longitudinal forces which generate motion, to all forces which resist the motion (especially to the lateral forces and longitudinal forces for non-driven wheels).

Therefore, in the analyzed case of control of robot motion, it is reasonable to introduce a higher level controller of velocity of the mobile platform, which works in addition to the wheel's velocity controller. Then, the desired velocities of spin of driven wheels are given by the following relationship:

$$\dot{\boldsymbol{\theta}}_d = \begin{bmatrix} \dot{\theta}_{ld} \\ \dot{\theta}_{rd} \end{bmatrix} = \frac{1}{r} \begin{bmatrix} 1 & -W/2 \\ 1 & W/2 \end{bmatrix} \mathbf{u}_v . \tag{18}$$

where $\mathbf{u}_v$ is a control signal at the output of the wheel's velocity controller, which is at the same time the input signal for the mobile platform velocity controller. This concept is presented in Fig. 4.

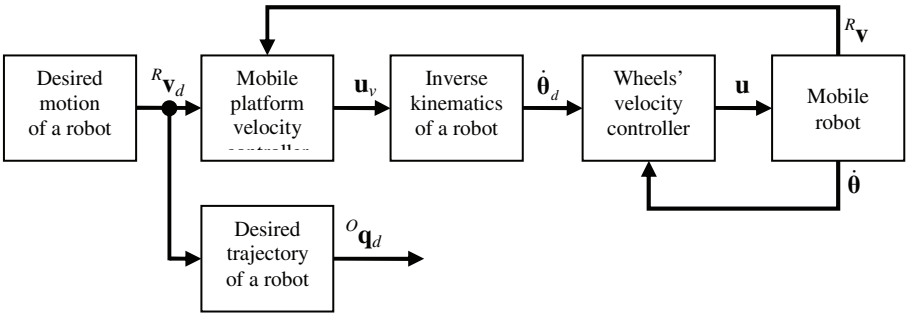

Fig. 4. Schematic diagram of robot motion control system with additional mobile platform velocity controller

Results of simulation investigations for both forms of the control system described above are presented in the work [14], whereas the results of empirical research in [15].

2.3 Dynamics of the Robot for Three Cases of the Drive System

For the needs of design and simulation of the control systems based on the object model (e.g., adaptive control), a simplified model of a four-wheeled mobile robot will be derived for the following drive system configurations:

- two out of four wheels of the robot are independently driven, that is, front or rear wheels,
- the same wheels of the robot as above are driven and drive is transmitted to the remaining two wheels via two tracks,
- all four robot wheels are independently driven.

It is assumed that robot is under action of the following external forces:

- ground reaction forces ${}^R\mathbf{F}_{Ai} = [{}^RF_{Aix}, {}^RF_{Aiy}, {}^RF_{Aiz}]^T$ acting on each wheel,
- gravity force ${}^R\mathbf{G} = m_R\, {}^R\mathbf{g}$, where m_R denotes total mass of the robot.

Reaction forces ${}^R\mathbf{F}_{Aix}$ and ${}^R\mathbf{F}_{Aiy}$, $i = \{1, 2, 3, 4\}$ acting in plane of wheel-ground contact are shown in Fig. 5. For simplicity, in further considerations the subscript A in designations of reaction forces and moments of reaction forces will be omitted.

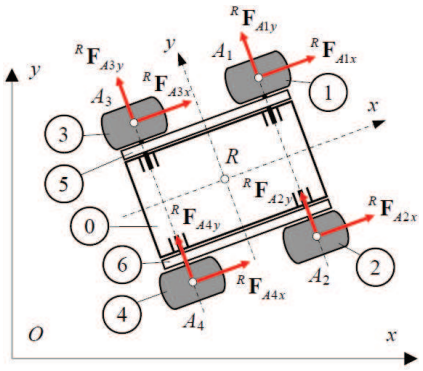

Fig. 5. Reaction forces acting on the PIAP SCOUT robot in the plane of wheel-ground contact

Force of gravity vector ${}^{R}\mathbf{G}$ is a function of gravitational acceleration vector ${}^{R}\mathbf{g} = [{}^{R}g_x, {}^{R}g_y, {}^{R}g_z]^T$ and it is applied at the robot mass center, whose position is described by the vector ${}^{R}\mathbf{r}_{CM} = [{}^{R}x_{CM}, {}^{R}y_{CM}, {}^{R}z_{CM}]^T$.

Under action of the mentioned forces, according to the Newton's 2nd law, the robot moves with acceleration ${}^{R}\mathbf{a}^{O}_{CM} = [{}^{R}a^{O}_{CMx}, {}^{R}a^{O}_{CMy}, {}^{R}a^{O}_{CMz}]^T$.

For all configurations of the robot drive system, the following dynamic equations of motion of the robot mass centre are valid:

$$m_R\,{}^{R}a^{O}_{CMx} = \sum_{i=1}^{4} {}^{R}F_{ix} + m_R\,{}^{R}g_x, \tag{19}$$

$$m_R\,{}^{R}a^{O}_{CMy} = \sum_{i=1}^{4} {}^{R}F_{iy} + m_R\,{}^{R}g_y, \tag{20}$$

$$m_R\,{}^{R}a^{O}_{CMz} = \sum_{i=1}^{4} {}^{R}F_{iz} + m_R\,{}^{R}g_z. \tag{21}$$

On the assumption that the robot does not rotate about *Rx* and *Ry* axes, it is possible to write the following two equations of equilibrium of moments of force about *R'x* and *R'y* axes, which are situated within the wheel-ground contact plane:

$$m_R({}^{R}a^{O}_{CMy} - {}^{R}g_y)(r + {}^{R}z_{CG}) + m_R\,{}^{R}g_z\,{}^{R}y_{CM} + ({}^{R}F_{1z} + {}^{R}F_{3z} - {}^{R}F_{2z} - {}^{R}F_{4z})W/2 = 0, \tag{22}$$

$$m_R(-{}^{R}a^{O}_{CMx} + {}^{R}g_x)(r + {}^{R}z_{CG}) - m_R\,{}^{R}g_z\,{}^{R}x_{CM} + ({}^{R}F_{3z} + {}^{R}F_{4z} - {}^{R}F_{1z} - {}^{R}F_{2z})L/2 = 0. \tag{23}$$

Taking into account the assumptions:

- the robot mobile platform is a rigid body,
- points of wheel-ground contact lie in one plane,
- wheel tires deflect directly proportional to reaction forces acting along direction normal to the ground and inversely proportional to their stiffnesses *k* (tire stiffnesses are assumed the same for all wheels),

one can write the following relationship for deflection of particular flexible wheels (with rubber tires):

$$(\Delta_3 - \Delta_1)/L = (\Delta_4 - \Delta_2)/L. \tag{24}$$

After substituting $\Delta_i = {}^R F_{iz}/k$ (because ${}^R F_{iz} = \Delta_i k$) additional equation is obtained:

$${}^R F_{3z} - {}^R F_{1z} = {}^R F_{4z} - {}^R F_{2z}. \tag{25}$$

On the assumption that the ground surface is horizontal and even as well as all wheels have contact with this surface, the gravitational acceleration vector expressed in the robot coordinate system $\{R\}$ is equal to: ${}^R\mathbf{g} = [0, 0, g]^T$, where $g = 9.81$ (m/s^2).

In this case, after putting ${}^R y_{CM} = 0$, based on equations (21), (22), (23) and (25) it is possible to determine normal components of reactions of the ground (on the assumption that accelerations of the robot mass center are known ${}^R a^O_{CMx}$, ${}^R a^O_{CMy}$, ${}^R a^O_{CMz}$, and ${}^R a^O_{CMz} = 0$) in the form:

$${}^R F_{1z} = m_R\left((-{}^R a^O_{CMx}/(2L) - {}^R a^O_{CMy}/(2W))(r + {}^R z_{CM}) + g(1/4 + {}^R x_{CM}/(2L))\right), \tag{26}$$

$${}^R F_{2z} = m_R\left((-{}^R a^O_{CMx}/(2L) + {}^R a^O_{CMy}/(2W))(r + {}^R z_{CM}) + g(1/4 + {}^R x_{CM}/(2L))\right), \tag{27}$$

$${}^R F_{3z} = m_R\left(({}^R a^O_{CMx}/(2L) - {}^R a^O_{CMy}/(2W))(r + {}^R z_{CM}) + g(1/4 - {}^R x_{CM}/(2L))\right), \tag{28}$$

$${}^R F_{4z} = m_R\left(({}^R a^O_{CMx}/(2L) + {}^R a^O_{CMy}/(2W))(r + {}^R z_{CM}) + g(1/4 - {}^R x_{CM}/(2L))\right). \tag{29}$$

For calculation of values of normal components of ground reaction forces, knowledge of motion parameters of the robot mass center *CM* and of geometric centers of wheels, that is, characteristic points *Ai*, is necessary. In the calculations, values of those parameters from the previous calculation step, that is, from time instant $t - \Delta t$, where Δt is the adopted time step, are used. In the first calculation step, known initial conditions are taken into account.

Current value of longitudinal slip factor for the *i*-th wheel is determined from the formula:

$$\lambda_i = \begin{cases} 0 \quad \text{for} \quad {}^{Ai} v^O_x = 0 \text{ and } v_{oi} = 0, \\ ({}^{Ai} v^O_x - v_{oi})/\max({}^{Ai} v^O_x, v_{oi}) \quad \text{for other} \quad {}^{Ai} v^O_x \text{ and } v_{oi}, \end{cases} \tag{30}$$

where $v_{oi} = \dot{\theta}_i r_i$ and ${}^{Ai} v^O_x$ are respectively velocity at the wheel circumference and longitudinal component of velocity of wheel geometric center.

Current value of the tire adhesion coefficient on longitudinal direction for this wheel is calculated using Kiencke tire model [12] modified by the author, that is, from the formula:

$$\mu_{ix} = \begin{cases} \dfrac{2\mu_p \lambda_p \lambda_i}{\lambda_p^2 + \lambda_i^2} \quad \text{for} \quad |\lambda_i| \le \lambda_p, \\ a_{\lambda x}\lambda_i + b_{\lambda x}\operatorname{sgn}(\lambda_i) \quad \text{for} \quad |\lambda_i| > \lambda_p, \end{cases} \tag{31}$$

where λ_p denotes the value of longitudinal slip corresponding to the value of maximum tire adhesion coefficient μ_p (Fig. 6).

Modification of the original Kiencke dependency is connected with calculation of the tire adhesion coefficient for $|\lambda_i| > \lambda_p$. The $\mu_{ix}(\lambda_i)$ characteristics is approximated by straight lines, so that, for longitudinal slip equal to +/–100%, the adhesion coefficient factor reaches a value corresponding to the sliding tire adhesion coefficient.

Coefficients $a_{\lambda x}$ and $b_{\lambda x}$ in (31) are described by formulas:

$$a_{\lambda x} = \frac{\mu_p - \mu_k}{\lambda_p - \lambda_{max}}, \qquad b_{\lambda x} = \mu_p - a_x \lambda_p, \tag{32}$$

where μ_k denotes sliding tire adhesion coefficient (identical to coefficient of kinetic friction), and $\lambda_{max} = 100\%$ is a maximum value of the longitudinal slip analyzed in the present work.

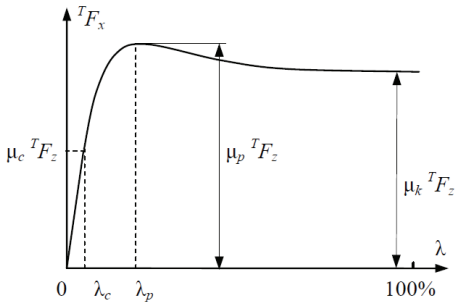

Fig. 6. Longitudinal force vs. longitudinal slip dependency for a rubber tire [18]

Longitudinal component of ground reaction force for the *i*-th wheel depends on current value of the adhesion coefficient on longitudinal direction, according to relationship:

$$^{R}F_{ix} = \mu_{ix}\ ^{R}F_{iz}. \tag{33}$$

In turn, the current value of the lateral slip angle for *i*-th wheel is determined from the formula:

$$\alpha_i = \begin{cases} 0 & \text{for} \quad {}^{Ai}v_y^O = 0, \\ \arctan 2({}^{Ai}v_y^O, |{}^{Ai}v_x^O|) & \text{for} \quad |{}^{Ai}v_x^O| > 0, \end{cases} \tag{34}$$

where ${}^{Ai}v_x^O$ and ${}^{Ai}v_y^O$ are respectively longitudinal and transversal velocity of the geometric center of the *i*-th wheel.

Knowing the lateral slip angle it is possible to calculate current value of the adhesion coefficient on lateral direction for *i*-th wheel. To this end the following approximate relationship (as compared to H.B. Pacejka model [10]) is introduced:

$$\mu_{iy} = -\mu_{ymax} \sin(\alpha_i), \tag{35}$$

where μ_{ymax} denotes maximum value of adhesion coefficient on lateral direction (it is assumed that $\mu_p \geq \mu_{ymax} \geq \mu_k$).

Hence, lateral component of the ground reaction force for *i*-th wheel is calculated from the formula:

$$ {}^{R}F_{iy} = \mu_{iy}\, {}^{R}F_{iz}. \tag{36} $$

For known components of longitudinal and lateral components of ground reaction forces for particular wheels, it is possible to calculate values of accelerations on longitudinal and lateral direction using equations (19) and (20):

$$ {}^{R}a^{O}_{CMx} = \sum_{i=1}^{4} {}^{R}F_{ix} / m_R, \tag{37} $$

$$ {}^{R}a^{O}_{CMy} = \sum_{i=1}^{4} {}^{R}F_{iy} / m_R. \tag{38} $$

For the robot mobile platform, it is also possible to write the following dynamic equation of motion resulting from its rotation about *Rz* axis with angular acceleration ${}^{R}\ddot{\varphi}^{O}_{0z}$:

$$ \begin{aligned} I_{Rz}\, {}^{R}\ddot{\varphi}^{O}_{0z} = \sum_{i=1}^{4} {}^{R}T_{iz} - ({}^{R}F_{1x} + {}^{R}F_{3x})(W/2 - {}^{R}y_{CM}) + ({}^{R}F_{2x} + {}^{R}F_{4x})(W/2 + {}^{R}y_{CM}) + \\ + ({}^{R}F_{1y} + {}^{R}F_{2y})(L/2 - {}^{R}x_{CM}) - ({}^{R}F_{3y} + {}^{R}F_{4y})(L/2 + {}^{R}x_{CM}), \end{aligned} \tag{39} $$

where: I_{Rz} – mass moment of inertia of the robot about the *Rz* axis, ${}^{R}T_{iz}$ – the so-called self-aligning torque associated with rotation of the *i*-th wheel about *Rz* axis, resulting from friction forces acting in the tire-ground contact.

After making assumption that ${}^{R}T_{iz} \approx 0$, that is, the self-aligning torque is negligibly small in comparison to the remaining moments of force acting about the *Rz* axis, and using equation (39) it is possible to determine value of the angular acceleration associated with robot rotation about *Rz* axis in the form:

$$ \begin{aligned} {}^{R}\ddot{\varphi}^{O}_{0z} = \Big(-({}^{R}F_{1x} + {}^{R}F_{3x})(W/2 - {}^{R}y_{CM}) + ({}^{R}F_{2x} + {}^{R}F_{4x})(W/2 + {}^{R}y_{CM}) + \\ + ({}^{R}F_{1y} + {}^{R}F_{2y})(L/2 - {}^{R}x_{CM}) - ({}^{R}F_{3y} + {}^{R}F_{4y})(L/2 + {}^{R}x_{CM})\Big) / I_{Rz}, \end{aligned} \tag{40} $$

and then calculate, by integration, the value of angular velocity of the robot mobile platform about this axis, that is ${}^{R}\dot{\varphi}^{O}_{0z}$.

Next, based on equations (11) it is possible to calculate values of velocities ${}^{R}v^{O}_{Rx}$ and ${}^{R}v^{O}_{Ry}$. In turn, after using equation (12) one can determine values of velocities of characteristic points *Ai*. To do so, one may assume that ${}^{R}x_C = {}^{R}x_B = 0$, that is the *x* coordinate describing position of the instantaneous centre of rotation for the mobile platform in the robot coordinate system $\{R\}$ is equal to 0.

For each of the robot wheels it is then possible to write dynamic equation of motion associated with wheel spin:

$$ I_{Wy}\, \ddot{\theta}_i = \tau_i + {}^{R}T_{ti} - {}^{R}F_{ix} r - {}^{R}F_{iz} r\, f_r\, \mathrm{sgn}(\dot{\theta}_i) - \tau_f\, \mathrm{sgn}(\dot{\theta}_i), \tag{41} $$

where: I_{Wy} – mass moment of inertia of the wheel about its spin axis, τ_i – a driving torque, τ_f – a torque of friction forces in a kinematic pair, ${}^R T_{ti}$ – a moment of force in the toothed belt, f_r – coefficient of rolling resistance, $\dot{\theta}_i$ and $\ddot{\theta}_i$ – angular velocity and acceleration of spin of that wheel, respectively.

In place of the signum function $\operatorname{sgn}(\dot{\theta}_i)$, one may introduce a $\tanh(k_\theta \dot{\theta}_i)$ function, which is better from the point of view of simulation, where the coefficient $k_\theta > 0$ should be the larger, the more the function should be similar to $\operatorname{sgn}(\dot{\theta}_i)$.

Moments of force τ_i and ${}^R T_{ti}$ depend on configuration of the robot drive system:

- for independent driving of rear wheels:

$$ {}^R T_{ti} = 0, \quad \tau_p = 0, \quad p = \{1, 2\}, \tag{42}$$

- for the hybrid drive system (i.e., with toothed belts):

$$ {}^R T_{tp} = \tau_a/2, \quad {}^R T_{ta} = -\tau_a/2, \quad a = \{3, 4\}, \quad p = \{1, 2\}, \tag{43}$$

- for independent driving of all four wheels:

$$ {}^R T_{ti} = 0, \quad i = a = \{1, 2, 3, 4\}, \tag{44}$$

where the subscript a is valid for driven wheels, and the subscript p for free wheels.

After taking into account the above relationships, it is possible to determine the following quantities from equation (41):

- driving torques τ_a for the driven wheels, based on desired angular parameters of their spin, i.e., $\dot{\theta}_a$ and $\ddot{\theta}_a$ (inverse dynamics problem) and angular parameters of rotation of free wheels, that is, $\dot{\theta}_p$ and $\ddot{\theta}_p$ (in case they are available);
- angular parameters of wheel spin, i.e., $\dot{\theta}_i$ and $\ddot{\theta}_i$ based on driving torques τ_a acting on the driven wheels (forward dynamics problem).

Eventually, the following solutions are obtained:

- for independent driving of either rear or front wheels:

$$ \tau_a = I_{Wy} \ddot{\theta}_a + \tau_f \operatorname{sgn}(\dot{\theta}_a) + {}^R F_{ax} r + {}^R F_{az} r f_r \operatorname{sgn}(\dot{\theta}_a), \tag{45}$$

$$ \ddot{\theta}_a = \left(\tau_a - {}^R F_{ax} r - {}^R F_{az} r f_r \operatorname{sgn}(\dot{\theta}_a) - \tau_f \operatorname{sgn}(\dot{\theta}_a)\right) / I_{Wy}, \tag{46}$$

$$ \ddot{\theta}_p = \left(- {}^R F_{px} r - {}^R F_{pz} r f_r \operatorname{sgn}(\dot{\theta}_p) - \tau_f \operatorname{sgn}(\dot{\theta}_p)\right) / I_{Wy}, \tag{47}$$

- for the hybrid drive system (with toothed belts):

$$ \tau_a = \tau_p = 2\left(I_{Wy} \ddot{\theta}_a + \tau_f \operatorname{sgn}(\dot{\theta}_a) + {}^R F_{ax} r + {}^R F_{az} r f_r \operatorname{sgn}(\dot{\theta}_a)\right), \tag{48}$$

$$ \ddot{\theta}_a = \left(\tau_a / 2 - {}^R F_{ax} r - {}^R F_{az} r f_r \operatorname{sgn}(\dot{\theta}_a) - \tau_f \operatorname{sgn}(\dot{\theta}_a)\right) / I_{Wy}, \tag{49}$$

$$\ddot{\theta}_p = \left(\tau_a / 2 - {}^R F_{px} r - {}^R F_{pz} r\, f_r \operatorname{sgn}(\dot{\theta}_p) - \tau_f \operatorname{sgn}(\dot{\theta}_p)\right) / I_{Wy}, \tag{50}$$

- for independent driving of all four wheels:

$$\tau_a = I_{Wy}\, \ddot{\theta}_a + \tau_f \operatorname{sgn}(\dot{\theta}_a) + {}^R F_{ax} r + {}^R F_{az} r\, f_r \operatorname{sgn}(\dot{\theta}_a), \tag{51}$$

$$\ddot{\theta}_a = \left(\tau_a - {}^R F_{ax} r - {}^R F_{az} r\, f_r \operatorname{sgn}(\dot{\theta}_a) - \tau_f \operatorname{sgn}(\dot{\theta}_a)\right) / I_{Wy}. \tag{52}$$

The above equations for torques τ_a can be written for all driven wheels in the compact form, better suited for synthesis of control systems:

$$\mathbf{Y}\,\mathbf{a} = \boldsymbol{\tau}, \tag{53}$$

where **a** is a vector of parameters of the dynamics model of the robot, and the matrix **Y** depends on current robot motion parameters.

In order to make the process of development of control systems easier, the model of robot dynamics should be linear with respect to the vector of robot parameters **a**.

For this reason, one may assume for simplification, that the adhesion coefficient μ_{ix} for tire and ground varies according to the Kiencke model [12], that is, based on the formula:

$$\mu_{ix} = 2\mu_p \lambda_p \lambda_i / (\lambda_p^2 + \lambda_i^2). \tag{54}$$

Equation (53) can be written in expanded form for the PIAP SCOUT robot [19] with hybrid drive system, in which rear wheels are driven, in the form of two scalar equations:

$$\begin{aligned} &2\left(a_1 \ddot{\theta}_3 + a_2 \operatorname{tgh}(k_{\dot{\theta}} \dot{\theta}_3) + 2\lambda_p \lambda_3 / (\lambda_p^2 + \lambda_3^2)(a_3 + a_4 {}^R a_{Rx}^O - a_5 {}^R a_{Ry}^O) + \right. \\ &\left. + (a_6 + a_7 {}^R a_{Rx}^O - a_8 {}^R a_{Ry}^O) \operatorname{tgh}(k_{\dot{\theta}} \dot{\theta}_3)\right) = \tau_3, \end{aligned} \tag{55}$$

$$\begin{aligned} &2\left(a_1 \ddot{\theta}_4 + a_2 \operatorname{tgh}(k_{\dot{\theta}} \dot{\theta}_4) + 2\lambda_p \lambda_4 / (\lambda_p^2 + \lambda_4^2)(a_3 + a_4 {}^R a_{Rx}^O + a_5 {}^R a_{Ry}^O) + \right. \\ &\left. + (a_6 + a_7 {}^R a_{Rx}^O + a_8 {}^R a_{Ry}^O) \operatorname{tgh}(k_{\dot{\theta}} \dot{\theta}_4)\right) = \tau_4, \end{aligned} \tag{56}$$

where the parameters of the robot dynamics model, which occur in equations, are equal to:

$$a_1 = b_1 = I_{Wy}, \qquad a_2 = b_2 = \tau_f, \tag{57}$$

$$a_3 = b_3 b_4 = \mu_p m_R g\, r(1/4 - {}^R x_{CM} / (2L)), \quad a_4 = b_3 b_5 = \mu_p m_R r(r + {}^R z_{CM}) / (2L), \tag{58}$$

$$a_5 = b_3 b_6 = \mu_p m_R r(r + {}^R z_{CM}) / (2W), \quad a_6 = b_4 b_7 = m_R g\, r(1/4 - {}^R x_{CM} / (2L)) f_r, \tag{59}$$

$$a_7 = b_5 b_7 = m_R r(r + {}^R z_{CM}) / (2L) f_r \qquad a_8 = b_6 b_7 = m_R r(r + {}^R z_{CM}) / (2W) f_r, \tag{60}$$

and:

$$b_3 = \mu_p, \quad b_4 = m_R g\, r(1/4 - {}^R x_{CM} / (2L)), \quad b_5 = m_R r(r + {}^R z_{CM}) / (2L), \tag{61}$$

$$b_6 = m_R r(r + {}^R z_{CM})/(2W), \quad b_7 = f_r. \tag{62}$$

Additionally, in place of $\mathrm{sgn}(\dot{\theta}_i)$ function one introduces the $\mathrm{tgh}(k_{\dot{\theta}}\dot{\theta}_i)$ function.

Based on the known parameters a_3–a_8, values of components of normal and longitudinal (for the driven wheels) ground reaction forces can be calculated in the form:

$${}^R F_{1z} = (a_6 - a_7\, {}^R a^O_{Rx} - a_8\, {}^R a^O_{Ry})/(r f_r), \quad {}^R F_{2z} = (a_6 - a_7\, {}^R a^O_{Rx} + a_8\, {}^R a^O_{Ry})/(r f_r), \tag{63}$$

$${}^R F_{3z} = (a_6 + a_7\, {}^R a^O_{Rx} - a_8\, {}^R a^O_{Ry})/(r f_r), \quad {}^R F_{4z} = (a_6 + a_7\, {}^R a^O_{Rx} + a_8\, {}^R a^O_{Ry})/(r f_r), \tag{64}$$

$${}^R F_{3x} = \mu_{3x}\, {}^R F_{3z} = 2\lambda_p \lambda_3/(\lambda_p^2 + \lambda_3^2)(a_3 + a_4\, {}^R a^O_{Rx} - a_5\, {}^R a^O_{Ry})/r, \tag{65}$$

$${}^R F_{4x} = \mu_{4x}\, {}^R F_{4z} = 2\lambda_p \lambda_3/(\lambda_p^2 + \lambda_3^2)(a_3 + a_4\, {}^R a^O_{Rx} + a_5\, {}^R a^O_{Ry})/r. \tag{66}$$

on condition that values of parameters r, f_r and μ_{ix} are known.

During analysis of equations (55)–(56) it can be noticed that for estimation of driving torques τ_3 and τ_4 for the configuration of the robot with the hybrid drive system, knowledge of values of the robot motion parameters like $\ddot{\theta}_3, \dot{\theta}_4, \ddot{\theta}_3, \ddot{\theta}_4, {}^R a^O_{Rx}, {}^R a^O_{Ry}$ and of wheel slips λ_3 and λ_4 (that follow from the previous quantities) are necessary. In those equations neither the angular acceleration ${}^R\ddot{\varphi}^O_{0z}$ of mobile platform rotation nor the mass moment of inertia I_{Rz} occur explicitly. Those quantities, however, affect other motion parameters of the robot.

2.4 Model of Friction in Kinematic Pairs

In research works usually the phenomenon of friction in robot kinematic pairs, e.g. in axles of wheels, is neglected, which is justified by small influence of this friction on robot motion. However, this influence becomes important for small velocities of robot motion, especially at the start and end of motion. In this case, the phenomenon of friction in kinematic pairs can lead to development of moments of values similar to the values of driving torques.

In the robot kinematic pairs the continuously differentiable friction model described in [9] may be used. According to it, the friction coefficient is assumed to have the following non-linear parameterizable form:

$$f_i = \gamma_{i.1}\left(\tanh(\gamma_{i.2}\dot{\theta}_i) - \tanh(\gamma_{i.3}\dot{\theta}_i)\right) + \gamma_{i.4}\tanh(\gamma_{i.5}\dot{\theta}_i) + \gamma_{i.6}\dot{\theta}_i, \tag{67}$$

where: $\gamma_{i.j}$ – positive constant parameters, i – kinematic pair number, $i = \{1,2,3,4\}$, j – parameter number, $j = \{1,2,...,6\}$, and the unit of $\dot{\theta}_i$ is (rad/s).

The static coefficient of friction μ_{si} is approximated by the term: $\gamma_{i.1} + \gamma_{i.4}$ whereas the kinetic one, i.e., μ_{ki} equals to $\gamma_{i.4}$. The term $\tanh(\gamma_{i.2}\dot{\theta}_i) - \tanh(\gamma_{i.3}\dot{\theta}_i)$ captures the Stribeck effect where the friction coefficient decreases from the static coefficient of friction with increasing slip velocity near the origin. A viscous dissipation term is given by $\gamma_{i.6}\dot{\theta}_i$. The Coulomb friction coefficient is modeled by the term $\gamma_{i.4}\tanh(\gamma_{i.5}\dot{\theta}_i)$. [9]

The friction torques in kinematic pairs are determined from the following relationship:

$$\tau_{fi} = -\|\mathbf{R}_i\| r_{fi} f_i , \tag{68}$$

where: $\|\mathbf{R}_i\|$ – magnitude of reaction force in the kinematic pair, r_{fi} – radius of friction in the kinematic pair.

2.5 Model of Robot Drive Units

The described simplified model of robot dynamics can be also enhanced with the model of its drive units. It is particularly important, when one wants to connect the model of robot dynamics (treated as a multi-body system) with a control system. In such case the drive unit model is an intermediate link between the control system and the robot dynamics model. The drive unit model can be used for solution of both forward and inverse dynamics problems.

It is assumed that:

- each of the robot drive units consists of identical DC motor, encoder, and transmission system,
- robot drive units are not self-locking, that is, they can freely turn under the influence of external moments of force,
- mass moments of inertia of the rotating elements of the servomechanisms (DC motor, encoder and gear unit) are small in comparison to mass moments of inertia of the driven parts of the robot (wheels), that is why they are neglected.

The DC motor model of the i^{th} drive unit is described by the following dependences:

$$\frac{\mathrm{d}i_i}{\mathrm{d}t} = \left(u_i - k_e n_d \dot{\theta}_i - R_d i_i\right) / L_d , \tag{69}$$

$$\tau_i = \eta_d n_d k_m i_i , \tag{70}$$

where: u_i – motor voltage input, i_i – rotor current, L_d, R_d – respectively inductance and resistance of the rotor, k_e – electromotive force constant, k_m – motor torque coefficient, n_d – gear ratio of the transmission system, η_d – efficiency factor of the transmission system.

After transforming the above equations to the form:

$$i_i = \tau_i / (\eta_d n_d k_m) , \tag{71}$$

$$u_i = k_e n_d \dot{\theta}_i + L_d \frac{\mathrm{d}i_i}{\mathrm{d}t} + R_d i_i , \tag{72}$$

one can also determine current flowing in the armature winding and the value of motor input voltage necessary for realization of motion of the wheel with desired angular velocity and with desired driving torque exerted by the wheel.

3 Conclusions and Future Works

In the present work the dynamics model of the four-wheeled robot with non-steered wheels is presented for three versions of the drive system. The most attention is devoted to the robot configuration with the hybrid drive system.

The robot model was developed based on results of empirical investigations of PIAP SCOUT robot [19] presented, for example, in works [14, 15].

As a part of this publication, author makes available the robot model implemented in the Matlab/Simulink environment, whose parameters were assumed for the version of the PIAP SCOUT robot [19] with hybrid drive system in which rear wheels are driven ([20] website).

Future works will include application of the robot dynamics model in synthesis and investigations of control systems, including those based on robot dynamics model.

Acknowledgements. The work has been realized as a part of the project entitled "Dynamics modeling of a four-wheeled mobile robot and tracking control of its motion with limitation of wheels slip". The project is financed from the means of National Science Centre of Poland granted on the basis of decision number DEC-2011/03/B/ST7/02532.

References

1. Barbosa de Oliveira Vaz, D.A., Inoue, R.S., Grassi Jr., V.: Kinodynamic Motion Planning of a Skid-Steering Mobile Robot Using RRTs. In: 2010 Latin American Robotics Symposium and Intelligent Robotics Meeting (2010)
2. Dąbek, P., Szosland, A.: Identification of rotational properties of a non-pneumatic tyre of a mobile robot. Pomiary Automatyka Robotyka 2(2011), 495–503 (2011) (in Polish: Identyfikacja parametrów skrętnych opony niepneumatycznej robota mobilnego)
3. Hendzel, Z.: An adaptive critic neural network for motion control of a wheeled mobile robot. Nonlinear Dynamics 50, 849–855 (2007)
4. Hua, J., et al.: Modeling and Control of Wheeled Mobile Robot in Constrained Environment Based on Hybrid Control Framework. In: Proceedings of the 2009 IEEE International Conference on Robotics and Biomimetics, Guilin, China (2009)
5. Iagnemma, K., Dubowsky, S.: Mobile Robots in Rough Terrain. Estimation, Motion Planning, and Control with Application to Planetary Rovers. STAR, vol. 12. Springer, Heidelberg (2004)
6. Kasprzyczak, L., Trenczek, S., Cader, M.: Robot for monitoring hazardous environments as a mechatronic product, Journal of Automation. Mobile Robotics & Intelligent Systems 6(4), 57–64 (2012)
7. Kozłowski, K., Pazderski, D.: Practical stabilization of 4WD skid-steering mobile robot – A kinematic-based Approach. In: 2006 IEEE 3rd International Conference on Mechatronics, Budapest, pp. 519–524 (2006)
8. Lenain, R., et al.: Mobile robot control in presence of sliding - Application to agricultural vehicle path tracking. In: Proceedings of the 45th IEEE Conference on Decision & Control, Manchester Grand Hyatt Hotel, San Diego, CA, USA (2006)

9. Makkar, C., Dixon, W.E., Sawyer, W.G., Hu, G.: A New Continuously Differentiable Friction Model for Control Systems Design. In: IEEE/ASME International Conference on Advanced Intelligent Mechatronics, Monterey, California, USA (2005)
10. Pacejka, H.B.: Tire and Vehicle Dynamics, 2nd edn. SAE International and Elsevier (2005)
11. Padhy, P.K., et al.: Modeling and Position Control of Mobile Robot. In: The 11th IEEE International Workshop on Advanced Motion Control, Nagaoka, Japan (2010)
12. Ping, L.Y.: Slip Modelling, Estimation and Control of Omnidirectional Wheeled Mobile Robots with Powered Caster Wheels. Doctorial Thesis, National University of Singapore, Singapore (2009)
13. Tian, Y., Sidek, N., Sarkar, N.: Modeling and control of a nonholonomic Wheeled Mobile Robot with wheel slip dynamics. In: IEEE Symposium on Computational Intelligence in Control and Automation, CICA 2009, pp. 7–14 (2009)
14. Trojnacki, M.: Dynamics modeling of wheeled mobile robots, OW PIAP, Warszawa (2013) (in Polish: Modelowanie dynamiki mobilnych robotów kołowych)
15. Trojnacki, M., Dąbek, P., Kacprzyk, J., Hendzel, Z.: Trajectory Tracking Control of a Four-Wheeled Mobile Robot with Yaw Rate Linear Controller. In: Szewczyk, R., Zieliński, C., Kaliczyńska, M. (eds.) Recent Advances in Automation, Robotics and Measuring Techniques. AISC, vol. 267, pp. 507–522. Springer, Heidelberg (2014)
16. Tu, C., et al.: Motion Control and Stabilization of a Skid-Steering Mobile Robot. In: 2nd International Conference on Adaptive Science & Technology, pp. 325–330 (2009)
17. Wang, D., Low, C.B.: Modeling and Analysis of Skidding and Slipping in Wheeled Mobile Robots - Control Design Perspective. IEEE Transactions on Robotics 24(3), 676–687 (2008)
18. Wong, J.Y.: Theory of Ground Vehicles, 3rd edn. Wiley-Interscience (2001)
19. Mobile robots for counter-terrorism (PIAP), http://www.antiterrorism.eu
20. Maciej, T.: Trojnacki: Mobile robots – models, animations and movies, http://www.mtrojnacki.republika.pl/MobileRobots/index.html